# ANALYSIS OF PERISTALTIC FLOW OF RABINOWITSCH FLUID IN A NON-UNIFORM CHANNEL: ANALYTICAL APPROACH

C. RAJASHEKHAR†, G. MANJUNATHA‡, HANUMESH VAIDYA§, K. V. PRASAD§, B. B. DIVYA‡ and J. SARASWATI§

†*Bhaskaracharya Study Chair, Karnataka State Akkamahadevi Women's University, Vijayapura-586108, Karnataka, India*

‡*Department of Mathematics, Manipal Institute of Technology, Manipal Academy of Higher Education, Manipal, Karnataka,576104, India*

§*Department of Mathematics, Vijayanagar Sri Krishnadevaraya University, Bellary, Karnataka, 583105, India*

*Corresponding Author: hanumeshvaidya@gmail.com*

***Abstract*— The present paper examines the impact of heat and mass transfer on the peristaltic flow of Rabinowitsch fluid flowing through a non-uniform channel. The effects of slip and variable fluid properties are taken into an account. The impacts of wall rigidity, wall stiffness, and viscous damping force parameter are considered. The equations governing the flow are rendered dimensionless by using a suitable similarity transformation. The governing equations of momentum, motion, energy, and concentration are solved by utilizing long wavelength and small Reynolds number approximation. The MATLAB 2019a programming has been used to obtain the solutions for velocity and concentration profiles. The series solution technique has been utilized to get the expression for temperature. The influence of relevant parameters on velocity, temperature, concentration, and streamlines are examined for viscous, shear thinning, and shear thickening fluid models. The examination uncovers that a rise in the value of variable viscosity and variable thermal conductivity improves the velocity and temperature profiles for Newtonian and pseudoplastic fluid models. Moreover, an increase in the volume of the trapped bolus is seen for an expansion in the estimation of the velocity slip parameter for all the three considered models.**

***Keywords*— velocity slip, thermal slip, concentration slip, wall rigidity, wall stiffness, viscous damping force parameter.**

## I. INTRODUCTION

Peristaltic flow is a mechanism induced by the area contraction and expansion, which travels along the wall of the flexible tube or channel, resulting in a sinusoidal wave. This mechanism has broad applications in the field of science and engineering. Notably, in the movement of food bolus through the esophagus, the urine movement in the ureter, movement of chyme in the gastrointestinal tract, the flow of spermatozoa in the cervical ducts of the male reproductive tract, the flow of blood through arteries involves the peristaltic movement. Further, this mechanism is also used in designing the peristaltic pump, heart-lung machine, and dialysis machines. The investigations on peristaltic transport have been initiated over the past few decades. Recently, the study of peristaltic transport using non-Newtonian fluids in different geometrical shapes has critical practical applications in many areas of science and technology. Furthermore, from the literature, it is evident that there exist very few studies on peristaltic transport of non-Newtonian fluids flowing through different configurations (Raju and Devanathan, 1972; Rajashekhar *et al*., 2018a).

The above examinations on the peristaltic transport were carried out in the absence of heat transfer. The examination of heat transfer is one of the significant research zones in synthetic designing, hemodialysis, and oxygenation, which has grabbed the attention of numerous researchers. The investigations on the impact of heat transfer on classical and biological liquids were carried out by numerous researchers (Oudina and Bessaih, 2016; Oudina and Makinde, 2018; Wakif *et al*., 2018; Vaidya *et al.*, 2019a; Wakif *et al.*, 2019; Das, 2019). Mass transfer is another significant phenomenon in understanding the dispersion of supplements from the blood to its adjacent tissues. In most of the mechanical applications, mass exchange assumes a considerable job in following the procedures associated with invert assimilation, film division process, dispersion of synthetic polluting influences, and refining process. The movements of heat and mass transfer impacts are viewed as together at that point; there exists a mind-boggling connection among motions and driving possibilities. Driven by the utilization of heat and mass transfer, a few scientists have examined the peristaltic movement with heat and mass transfer (Akram *et al*., 2014; Ramesh, 2016).

Most of the investigations on biological fluids are carried out by taking no-slip conditions into account. However, it is noticed that in examining the peristaltic transport, there exist a certain amount of slippage at the wall. This slip plays a vital role in reviewing the complex behavior of biological liquids. Further, the slip conditions also play a significant role in polymer industries where they exhibit a macroscopic wall slip. Motivated by the applications of slip conditions in biological and classical liquids, numerous researchers have investigated the impact of slip conditions through different geometries (Kumar and Seth, 2019; Bhatti and Zeeshan, 2016; Vaidya *et al*., 2018; Manjunatha *et al*., 2019a; Latha *et al.*, 2018).

The effects of wall properties such as wall rigidity, wall stiffness, and viscous damping force parameters have a critical role to play when it comes to biological liquids. Thus, the present study incorporates the effects of the wall along with variable liquid properties. Further, the usage of non-Newtonian fluids has been established to be the most prominent in comparison to the Newtonian fluids in industrial systems, medical science as well as engineering fields. As a result, many non-Newtonian fluid flow models have been used in studying the flow mechanism, such as power-law, Jeffrey fluid, UCM fluid, Dusty fluid, Bingham, Herschel-Bulkley, Casson, couple stress, Rabinowitsch fluid, etc. (Hayat *et al*., 2008; Javed *et al*., 2014; Rajashekhar *et al*., 2018b; Vaidya *et al*., 2019b; Manjunatha *et al*., 2019b; Vaidya *et al*., 2019c; Makinde and Reddy, 2019; Reddy *et al*., 2016; Reddy *et al*., 2018).

Inspired by the above examinations, the current investigation is carried out by utilizing a non-Newtonian Rabinowitsch model. This model assumes a primary job in understanding the sophisticated rheological practices of natural liquids. Since it is a cubic pressure model shows the qualities of shear thinning or pseudoplastic (e.g., ketchup, syrup, and blood plasma), shear thickening or dilatant (e.g., polyethylene glycol, oobleck, and sand) and Newtonian (e.g., water and air) liquids. Driven by the applications of non-Newtonian liquids and to the best of the author's knowledge, no attempts have made to discover the impact of external effects on the fluid flow. The present work investigates the heat transfer characteristics of non-Newtonian fluid flow under the influence of external forces through the non-uniform channel.

## II. METHODS

Consider a viscous incompressible fluid flowing through a non-uniform channel (See Fig. 1). The flow is governed by non-Newtonian Rabinowitsch liquid induced by the sinusoidal wave trains of wavelength $\lambda$. The sinusoidal wave train $h(x,t)$ travelling along the walls of the channel is given by

$$y = h(x,t) = a + b\sin\left(\frac{2\pi}{\lambda}(x-ct)\right) \tag{1}$$

with $a = a_0 + a_1 x$, where $a_0$ the half width of the channel, $a_1$ is constant ($a_1 \ll 1$), $c$ is the wave speed, $\lambda$ is the wavelength and $t$ is the time.

The equations governing the flow can be written as follows:

$$\frac{\partial u}{\partial x} + \frac{\partial v}{\partial y} = 0, \tag{2}$$

$$\rho\left(\frac{\partial u}{\partial t} + u\frac{\partial u}{\partial x} + v\frac{\partial u}{\partial y}\right) = -\frac{\partial p}{\partial x} + \frac{\partial \tau_{xx}}{\partial x} + \frac{\partial \tau_{xy}}{\partial y}, \tag{3}$$

$$\rho\left(\frac{\partial v}{\partial t} + u\frac{\partial v}{\partial x} + v\frac{\partial v}{\partial y}\right) = -\frac{\partial p}{\partial y} + \frac{\partial \tau_{xx}}{\partial x} + \frac{\partial \tau_{xy}}{\partial y}, \tag{4}$$

$$\rho c_p\left(\frac{\partial T}{\partial t} + u\frac{\partial T}{\partial x} + v\frac{\partial T}{\partial y}\right) = \frac{\partial}{\partial y}\left(k(t)\frac{\partial T}{\partial x}\right) + \frac{\partial}{\partial y}\left(k(t)\frac{\partial T}{\partial y}\right) + \tau_{xx}\frac{\partial u}{\partial x} + \tau_{yy}\frac{\partial v}{\partial y} + \tau_{xy}\left(\frac{\partial v}{\partial x} + \frac{\partial u}{\partial y}\right) = 0, \tag{5}$$

$$\frac{\partial C}{\partial t} + u\frac{\partial C}{\partial x} + v\frac{\partial C}{\partial y} = D_w\left(\frac{\partial^2 C}{\partial x^2} + \frac{\partial^2 C}{\partial y^2}\right) + \frac{D_m K_T}{T_m}\left(\frac{\partial^2 T}{\partial x^2} + \frac{\partial^2 T}{\partial y^2}\right) \tag{6}$$

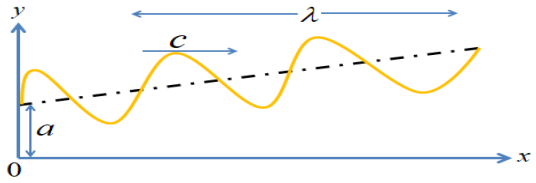


Fig. 1: Geometry of the peristaltic wave in a channel.

where $u$ and $v$ are the velocity components in axial and radial directions respectively, $\rho$ is the density of the fluid, $p$ is the pressure, $\tau_{xx}$, $\tau_{xy}$, $\tau_{yy}$ are extra stress components, $T$ is the temperature, $C$ is the concentration, $D_w$ is the coefficient of mass diffusivity, $k$ is the thermal conductivity, $K_T$ is the thermal diffusion ratio, $T_m$ is the mean fluid temperature and $c_p$ denote the specific heat at constant volume.

The equation of the flexible wall motion is expressed as

$$-\tau\frac{\partial^2}{\partial x^2} + n_1\frac{\partial^2}{\partial t^2} + n_2\frac{\partial}{\partial t} = p - p_0, \tag{7}$$

where $\tau$ is the elastic tension, $n_1$ is the mass per unit are and $n_2$ is the coefficient of wall damping force.

By using the $x$ component of momentum, the continuity of stress at $y = h$ is given by

$$\frac{\partial p}{\partial y} = \frac{\partial \tau_{xx}}{\partial x} + \frac{\partial \tau_{xy}}{\partial y} - \rho\left(\frac{\partial u}{\partial t} + u\frac{\partial u}{\partial x} + v\frac{\partial u}{\partial y}\right). \tag{8}$$

The non-dimensional quantities of interest are given below

$$x' = \frac{x}{\lambda},\ y' = \frac{y}{a},\ u' = \frac{u}{c},\ v' = \frac{v}{c\xi},\ h' = \frac{h}{a},\ c_p = \frac{a}{\lambda}, \tag{9}$$

$$p' = \frac{pa^2}{\mu_0\lambda c},\ \mathrm{Re} = \frac{ac}{\vartheta},\ \vartheta = \frac{\mu_0}{\rho},\ {\mu_0}' = \frac{\mu_0}{\mu},\ \varepsilon = \frac{b}{a},\ {\tau_{xx}}' = \frac{a\tau_{xx}}{\mu_0 c},$$

$${\tau_{xy}}' = \frac{a\tau_{xy}}{\mu_0 c},\ {\tau_{yy}}' = \frac{a\tau_{yy}}{\mu_0 c},\ \psi' = \frac{\psi}{ac},\ t' = \frac{tc}{\lambda},$$

$$E_1 = \frac{-\tau a^3}{\lambda\mu_0^3 c},\ \mathrm{Pr} = \frac{\mu_0 c_p}{k_0},\ Sr = \frac{\rho D_m K_T T_0}{T_w \mu_0 C_0},\ Sc = \frac{\mu_0}{\rho D_m},$$

$$E_2 = \frac{n_1 c a^3}{\lambda^3\mu_0},\ E_3 = \frac{n_2 a^3}{\lambda^3\mu_0},\ \theta = \frac{T-T_0}{T_0},\ N = Ec \times \mathrm{Pr},$$

$$Ec = \frac{c^2}{c_p T_0},\ \sigma = \frac{C'-C_0}{C_0},\ \gamma = \frac{\mu_0^2 c^2 \mu_1}{a^2}$$

On utilizing the non-dimensional transformations as mentioned above, the Eqs. (2)-(6) after applying the long wavelength and small Reynolds number takes the following form

$$\frac{\partial p}{\partial x} + \frac{\partial \tau_{xy}}{\partial y}, \tag{10}$$

$$\frac{\partial p}{\partial y} = 0, \tag{11}$$

$$\frac{\partial}{\partial y}\left(k(\theta)\frac{\partial \theta}{\partial y}\right) + N\tau_{xy}\left(\frac{\partial u}{\partial y}\right) = 0, \tag{12}$$

$$\frac{\partial^2 \sigma}{\partial y^2} + ScSr\frac{\partial^2 \theta}{\partial y^2} = 0, \tag{13}$$

where $\tau_{xy}$ is the constitutive equation of Rabinowitsch fluid and in the non-dimensional form, it is given by

$$\tau_{xy} + \gamma\tau_{xy}^3 = \mu(y)\frac{\partial u}{\partial y}, \tag{14}$$

where $\gamma$ is the coefficient of pseudoplasticity and $\mu$ is the fluid viscosity.

The corresponding non-dimensional boundary conditions are given by

$$u + \alpha\frac{\partial u}{\partial y} = -1, \theta + \alpha_1\frac{\partial \theta}{\partial y} = 0, \sigma + \alpha_2\frac{\partial \sigma}{\partial y} = 0\Big\} \tag{15}$$

$$\text{at } y = h = 1 + mx + \varepsilon\sin[2\pi(x-t)]$$

$$\frac{\partial u}{\partial y} = 0, \frac{\partial \theta}{\partial y} = 0, \frac{\partial \sigma}{\partial y} = 0 \text{ at } y = 0 \quad (16)$$

where $\alpha$, $\alpha_1$ and $\alpha_2$ are the velocity slip, thermal slip, and concentration slip respectively.

The variations in viscosity $\mu(y)$ and thermal conductivity $k(\theta)$ appearing in Eqs. (14) and (12) are defined as

$$\mu(y) = 1 - \beta y, \text{ for } \beta \ll 1, \quad (17)$$

$$k(\theta) = 1 + \phi\theta, \text{ for } \phi \ll 1, \quad (18)$$

where $\beta$ and $\phi$ are the viscosity and thermal conductivity coefficients.

## III. SOLUTION OF THE PROBLEM

The expression for velocity is obtained by solving Eq. (10) with the help of boundary conditions (15) and (16). The expression for velocity so obtained is given by

$$u = \frac{1}{6}\left\{-6 + \frac{6\alpha(hP+h^3P^3\gamma)}{-1+h\beta} + \right. \quad (19)$$

$$+ \frac{6hP\beta^3+hP^3\beta(6+h\beta(3+2h\beta))\gamma+6P(\beta^2+P^2\gamma)\log(1-h\beta)}{\beta^4} +$$

$$\left. + \frac{6yP\beta^3+yP^3\beta(6+y\beta(3+2y\beta))\gamma+6P(\beta^2+P^2\gamma)\log(1-y\beta)}{\beta^4}\right\}$$

Noting here that the $x$ components of the pressure gradient $P$ appearing in Eq. (19) and defined by Eq. (8) is simplified as follows

$$P = 4\pi^2\varepsilon\{-2\pi\cos[2\pi(x-t)](E_1+E_2) + \quad (20)$$

$$-2\pi\sin[2\pi(x-t)]E_3\}.$$

The stream function is obtained by using $u = \partial\psi/\partial y$ with the condition $\psi = 0$ at $y = 0$.

Due to the non-linearity in the Eq. (12), we cannot find an exact solution for the problem. Hence, we adopt the perturbation method to expand the temperature profile $\theta$ for the small value of variable thermal conductivity $\phi$

$$\theta = \theta_0 + \phi\theta_1 + O(\phi^2) \quad (21)$$

Substituting the Eq. (21) in Eq. (12) and making use of the boundary conditions (15) and (16), we obtain the expressions for temperature. Further, the expression for concentration is achieved by making use of the temperature equation. Following the same procedure, the expression for concentration can be obtained by using the temperature expression after performing lengthy calculations. The MATLAB code has been written to carry out the lengthy calculations involved in finding the solutions for temperature and concentration expressions.

The expressions for Skin friction coefficient $(c_f)$, Nusselt number $(Nu)$ and Sherwood number $(Sh)$ are as follows:

$$c_f = \frac{\delta h}{\delta x}\left(\frac{\delta u}{\delta y}\right)_{y=h} \quad (22)$$

$$Nu = \frac{\delta h}{\delta x}\left(\frac{\delta \theta}{\delta y}\right)_{y=h} \quad (23)$$

$$Sh = \frac{\delta h}{\delta x}\left(\frac{\delta \sigma}{\delta y}\right)_{y=h} \quad (24)$$

## IV. RESULTS AND DISCUSSION

This section emphasizes on the impacts of variable viscosity $(\beta)$, variable thermal conductivity $(\phi)$, velocity slip parameter $(\alpha)$, thermal slip parameter $(\alpha_1)$, concentration slip parameter $(\alpha_2)$, Brinkmann number $(N)$, Schmidt number $(Sc)$, Soret number $(Sr)$, the wall rigidity parameter $(E_1)$, the wall stiffness parameter $(E_2)$ and the viscous damping force parameter $(E_3)$ on velocity $(u)$, temperature $(\theta)$, concentration $(\sigma)$, Skin friction coefficient $(c_f)$, Nusselt number $(Nu)$, Sherwood number $(Sh)$ and streamlines $(\psi)$ are analyzed and discussed through graphs 2-9. Further, the MATLAB software has been utilized for the pictorial representations of relevant parameters of interest on physiological quantities with the fixed values of parameters.

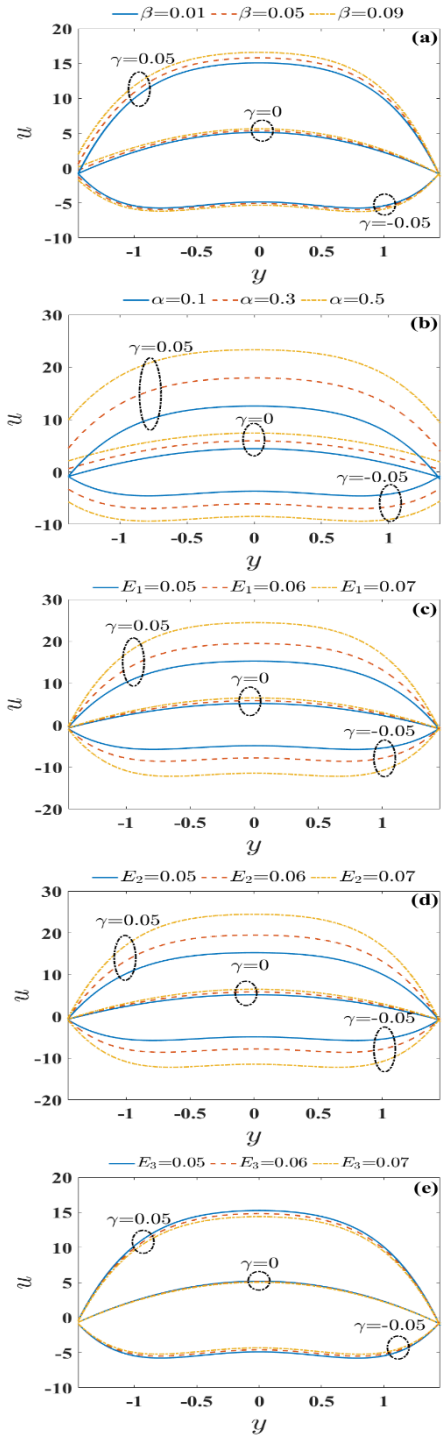


**Fig. 2**. Velocity profiles for varying (a) variable viscosity $(\beta)$, (b) velocity slip parameter $(\alpha)$, (c) wall rigidity parameter $(E_1)$, (d) wall stiffness parameter $(E_2)$ and (e) viscous damping force parameter $(E_3)$.

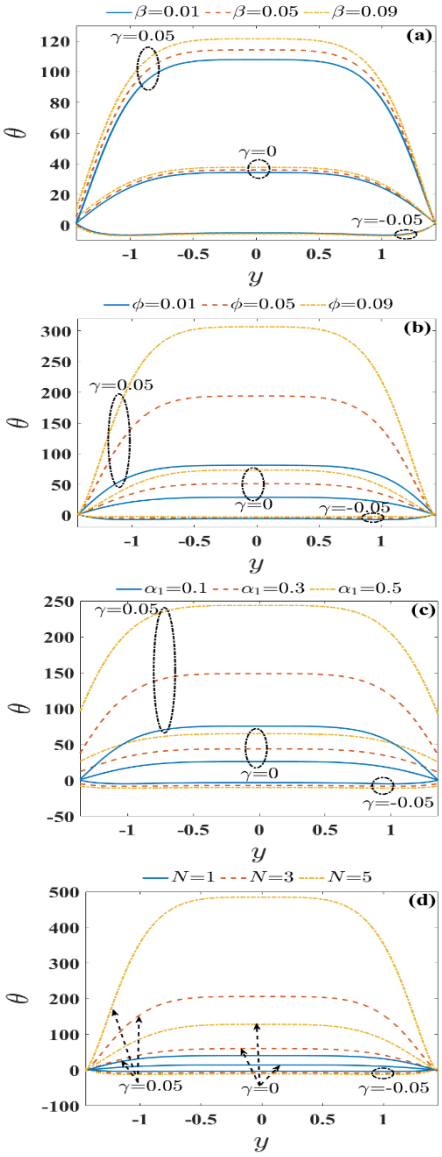


**Fig. 3.** Temperature profiles for varying (a) variable viscosity ($\beta$), (b) variable thermal conductivity ($\phi$), (c) thermal slip ($\alpha_1$) and (d) Brinkman number ($N$).

Figure 2 is drawn to see the impacts of variable viscosity, velocity slip, and wall properties (wall rigidity, wall stiffness, and viscous damping force parameter) on the velocity profiles. From the figure, it is evident that the maximum velocity occurs at the center of the channel. Figs. 2(a) and 2(b) shows that an increase in the value of variable viscosity and velocity slip parameter increases the velocity profiles for Newtonian and pseudoplastic fluids. Further, it is observed that the higher values of variable viscosity and velocity slip parameter diminishes the velocity profiles for dilatant liquid. Figs. 2(c)-(e) are portrayed to analyze the effects of $E_1$, $E_2$ and $E_3$ on velocity profiles for different fluids. From Fig. 2(a) and 2(b), the velocity is an increasing function of $E_1$ and $E_2$ for Newtonian and pseudoplastic fluid models. Whereas, it is a decreasing function of $E_1$ and $E_2$ for dilatant fluids. Furthermore, the impact of $E_3$ shows the opposite behavior as that of $E_1$ and $E_2$ on velocity profiles.

Figure 3 is sketched to analyze the impacts of appropriate parameters on temperature profiles. Figure 3(a) reveals that the temperature of viscous and shear thinning liquids drops due to the increase in the value of variable viscosity. However, the temperature profiles of shear thickening liquids diminish for larger estimations of variable viscosity. The impact of thermal conductivity enhances the temperature of all three liquids (See Fig. 3(b)). This is because of a rise in the value of thermal conductivity allows the fluid to scatter the heat to its surroundings. Thus, it increases the temperature of the liquid when compared to the boundary temperature, which results in increasing the temperature of all three fluids. Figure 3(c) demonstrates the impacts of thermal slip parameter on temperature profiles. Generally, the temperature profiles of dilatant liquid diminish for higher estimations of thermal slip parameter, whereas it enhances for Newtonian and pseudoplastic fluids. Figure 3(d) depicts the variation of Brinkman number on temperature profiles. The impact of Brinkmann number on temperature reveals that an increase in the value of Brinkmann number decreases the temperature profiles when $\gamma = -0.05$. Also note that when $\gamma = 0$ and $0.05$, the temperature profiles enhance for higher values of Brinkmann number. This is a direct result of higher estimations of Brinkmann number increases the viscous dissipation force and thereby enhances temperature profiles.

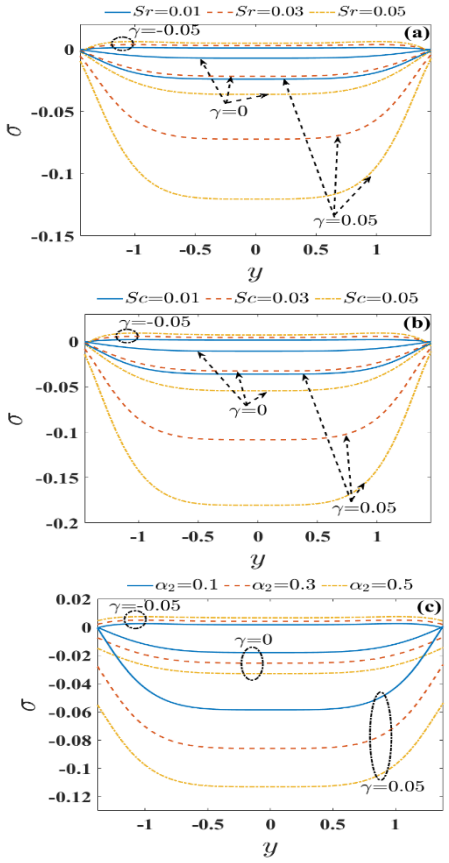


**Fig. 4.** Concentration profiles for varying (a) Soret number ($Sr$), (b) Schmidt number ($Sc$), (c) concentration slip parameter ($\alpha_2$).

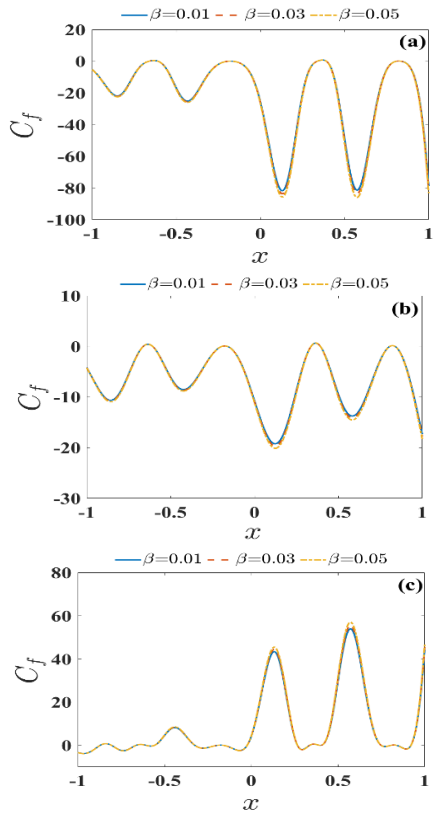


**Fig. 5.** Skin Friction coefficient for varying variable viscosity($\beta$) for (a) pseudoplastic fluid, (b) Newtonian fluid and (c) dilatant fluid.

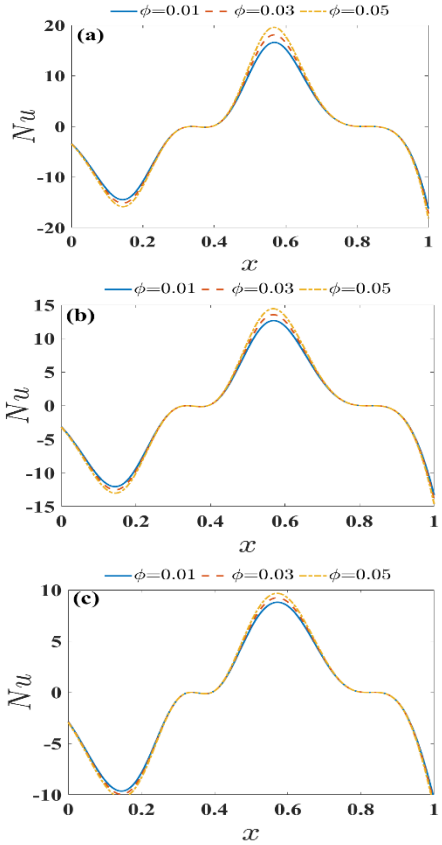


**Fig. 6.** Nusselt number for varying variable thermal conductivity ($\phi$) for (a) pseudoplastic fluid, (b) Newtonian fluid and (c) dilatant fluid.

The concentration profiles reveal the contrary impact as compared with the temperature profiles. This behavior is physically logical, as heat and mass are known to be inversely related. Moreover, it is clear from the patterns that the fluid particles are more concentrated near the channel walls than the central region. Biologically, this behavior is apparent as the essential nutrients from the blood and other fluids diffuse out to the adjacent cells and tissues.

Figure 4 is drawn to see the impact of pertinent parameters on the concentration profiles. From the figure it is noticed that an increase in the value of Soret and Schmidt number diminishes the concentration profile for viscous and shear thinning fluids, whereas the concentration profile enhances for shear thickening fluid (See Fig. 4(a) and 4(b)). Figure 4(c) is graphed to see the effect of concentration slip parameter on concentration profiles. From the figure, it is noticed that an increase in the value of concentration slip parameter enhances the concentration profiles for dilatant liquid, whereas the concentration profiles diminish for Newtonian and pseudoplastic fluid models.

Figure 5 shows the impact of variable fluid viscosity on skin friction coefficient. As seen from Figs. 5(a)-(c), the magnitude of the skin friction coefficient increases for the increasing values of the coefficient of variable viscosity for pseudoplastic, Newtonian as well as dilatant

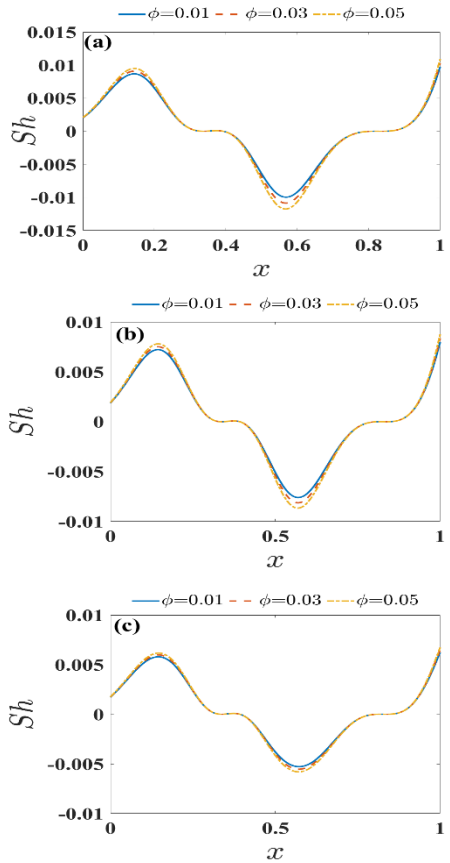


**Fig. 7.** Sherwood Number for varying variable thermal conductivity ($\phi$) for (a) pseudoplastic fluid, (b) Newtonian fluid and (c) dilatant fluid.

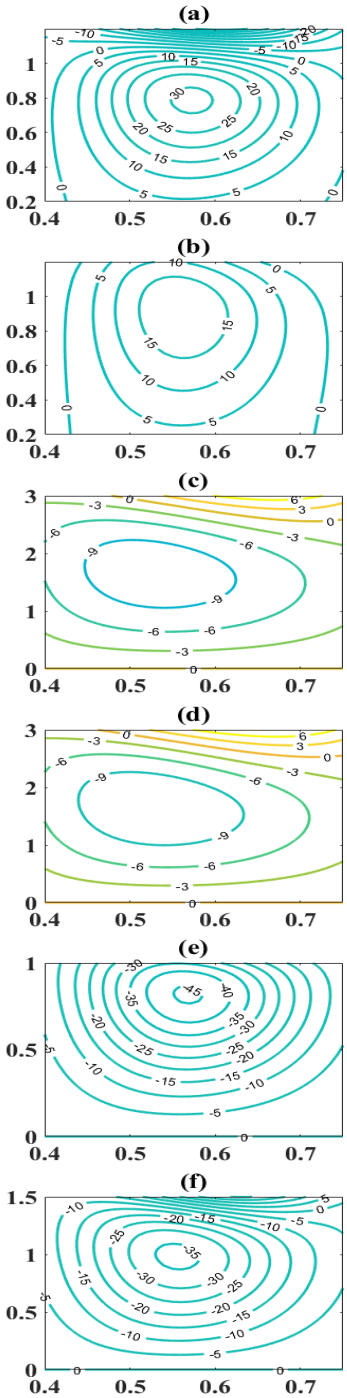


**Fig. 8.** Streamlines for varying (a) $\beta = 0.01$ and $\gamma = -0.05$, (b) $\beta = 0.02$ and $\gamma = -0.05$ (c) $\beta = 0.01$ and $\gamma = 0$, (d) $\beta = 0.02$ and $\gamma = 0$, (e) $\beta = 0.01$ and $\gamma = 0.05$ and (f) $\beta = 0.02$ and $\gamma = 0.05$.

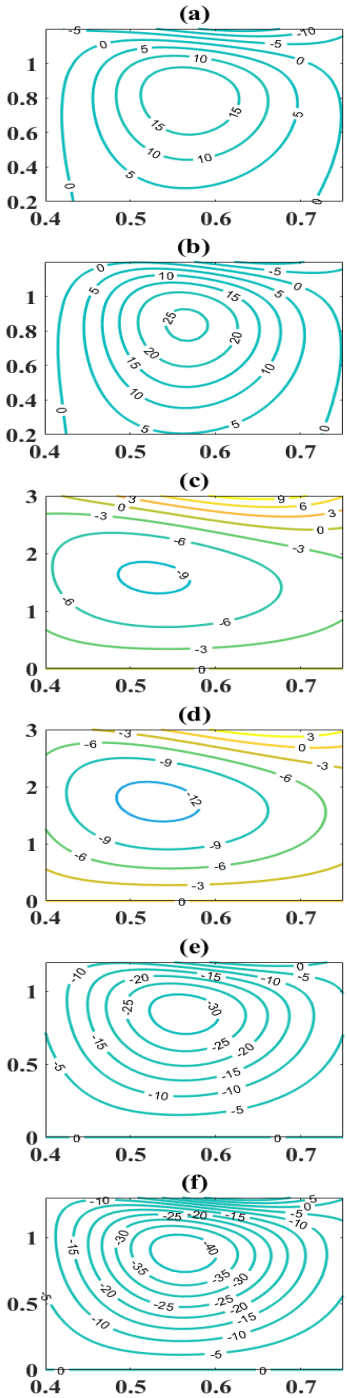


**Fig. 9.** Streamlines for varying (a) $\alpha = 0.1$ and $\gamma = -0.05$, (b) $\alpha = 0.2$ and $\gamma = -0.05$ (c) $\alpha = 0.1$and $\gamma = 0$, (d) $\alpha = 0.2$ and $\gamma = 0$, (e) $\alpha = 0.1$ and $\gamma = 0.05$ and (f) $\alpha = 0.2$ and $\gamma = 0.05$.

fluids. The influence of the coefficient of variable thermal conductivity on Nusselt number and Sherwood number are plotted in Figs. 6 and 7 respectively. These graphs indicate an increase in magnitude of Sherwood and Nusselt numbers for all the three types of fluids as the values of the coefficient of variable thermal conductivity increase.

The trapping is a remarkable phenomenon in understanding the flow characteristics of biological liquids such as in the movement of thrombus in blood vessels and the chyme movement in the gastrointestinal tract. Notably, the peristaltic mechanism involved in these systems helps us in analysing the formation and mobility of the bolus. Figures 8 and 9 are drawn to see the impact of variable viscosity and velocity slip parameters on the trapped bolus. From Fig. 8, it is noticed that an increase in the value of variable viscosity diminishes the size of trapped bolus for dilatant and

pseudoplastic fluid models, whereas it increases for Newtonian liquid. Figure 9 reveals that an increase in the value of the velocity slip parameter enhances the size of trapped bolus for all the three considered models.

## V. CONCLUSIONS

The present article inspects the impacts of variable liquid properties on the peristaltic mechanism of Rabinowitsch liquid. The effects of heat and mass exchange are contemplated through a non-uniform channel affected by slip and wall properties. The impacts of pertinent parameters on the physiological quantities of interest are presented graphically. The significant outcomes of the present article can be summed as:

- The presence of variable viscosity enhances the velocity profiles for Newtonian and pseudoplastic fluid models.
- The impact of velocity slip parameter diminishes the velocity profiles for dilatant liquid.
- The variable thermal conductivity is an increasing function of temperature for dilatant, Newtonian and pseudoplastic fluid models.
- The rise in concentration profile is observed for an increment in the value of concentration slip parameter for dilatant liquid.
- The Soret and Schmidt numbers cause a drop in the concentration profiles for viscous and pseudoplastic fluid models.
- The number of bolus formation enhances with an increase in the value of velocity slip parameter for all the three considered models.

## ACKNOWLEDGEMENT

The authors thank the valuable comments of the reviewers, which has helped in the improvement of this research article.

## REFERENCES

Akram, S., Nadeem, S. and Hussain, A. (2014). "Effects of heat and mass transfer on peristaltic flow of a Bingham liquid in the presence of inclined magnetic field and channel with different wave forms," *Journal of Magnetism and Magnetic Materials*, **362**, 184-192.

Bhatti, M.M. and Zeeshan, A. (2016). "Heat and mass transfer analysis on peristaltic flow of particle-fluid suspension with slip effects," *Journal of Mechanics in Medicine and Biology*, **17**, 1750028.

Das, U.J., (2019). "Soret and Dufour effects on three dimensional mixed convective hydromagnetic flow of a visco-elastic fluid past an infinite inclined plate," *Latin American Research*, **49**, 7-12.

Hayat, T., Javed, M. and Ali, N. (2008). "MHD peristaltic of a Jeffery fluid in a channel with compliant walls and porous space," *Transport in Porous Media*, **74**, 259-274.

Javed, M., Hayat, T. and Alsaedi, A. (2014). "Peristaltic flow of Burgers' fluid with compliant walls and heat transfer," *Applied Mathematics and Computation*, **244**, 654-671.

Kumar, B. and Seth, G.S. (2019). "MHD Stagnation point transient flow of nanofluid past a stretching sheet: SRM approach," *Latin American Applied Research*, **49**, 205-211.

Latha, R., Kumar, B.R. and Makinde, O.D. (2018). "Peristaltic flow of Couple stress fluid in an asymmetric channel with partial slip," *Defect and Diffusion Forum*, **387**, 385-402.

Makinde, O.D. and Reddy, M.G. (2019). "MHD peristaltic slip flow of Casson fluid and heat transfer in channel filled with a porous medium," *Scientia Iranica*, **26**, 2342-2355.

Manjunatha, G., Rajashekhar, C., Hanumesh, V., Prasad, K.V. and Makinde, O.D. (2019a). "Transport of Rabinowitsch Fluid through an Inclined Non-Uniform Slippery Tube," *Defect and Diffusion Forum*, **392**, 138-157.

Manjunatha, G., Rajashekhar, C., Vaidya, H. and Prasad, K.V. (2019b). "Peristaltic mechanism of Bingham liquid in a convectively heated porous tube in the presence of variable liquid properties," *Special Topics and Reviews in Porous Media- An International Journal*, **10**, 187-201.

Oudina, F.M. and Bessaih, R. (2016). "Oscillatory magnetohydrodynamic natural convection of liquid metal between vertical coaxial cylinders," *Journal of Applied Fluid Mechanics*, **9**, 1655-1665.

Oudina, F.M. and Makinde, O.D. (2018). "Numerical simulation of oscillatory MHD natural convection in cylindrical annulus: Prandtl number effect," *Defect and Diffusion Forum*, **387**, 417-427.

Rajashekhar, C., Manjunatha, G., Prasad, K.V., Baliga, B.B. and Vaidya, H. (2018a). "Peristaltic transport of two-layered blood flow using Herschel-Bulkley model," *Cogent Engineering*, **5**, 1-16.

Rajashekhar, C., Manjunatha, G., Vaidya, H., Divya, B. B., Prasad and K.V. (2018b). "Peristaltic flow of Casson liquid in an inclined porous tube with convective boundary conditions and variable liquid properties," *Frontiers in Heat and Mass Transfer*, **11**, 35.

Raju, K.K. and Devanathan, R. (1972). "Peristaltic motion of a non-Newtonian fluid," *Rheological Acta*, **11,** 170-178.

Ramesh, K. (2016). "Influence of heat and mass transfer on peristaltic flow of a couple stress fluid through porous medium in the presence of inclined magnetic field in an inclined asymmetric channel," *Journal of Molecular Liquids*, **219**, 256-271.

Reddy, K.V., Makinde, O.D. and Reddy, M.G. (2018). "Thermal analysis of MHD electro-osmotic peristaltic pumping of Casson fluid through a rotating asymmetric micro-channel," *Indian Journal of Physics*, **92**, 1439-1448.

Reddy, M.G., Reddy, K.V. and Makinde, O.D. (2016). "Hydromagnetic peristaltic motion of a reacting and

radiating couple stress fluid in an inclined asymmetric channel filled with a porous medium," *Alexandria Engineering Journal*, **55**, 1841-1853.

Vaidya, H., Manjunatha, G., Rajashekhar, C. and Prasad, K.V. (2018). "Role of slip and heat transfer on peristaltic transport of Herschel-Bulkley fluid through an elastic tube," *Multidiscipline Modelling in Materials and Structures*, **14**, 940-959.

Vaidya, H., Rajashekhar, C., Manjunatha, G. and Prasad, K.V. (2019a). "Effects of Heat Transfer on Peristaltic Transport of a Bingham Fluid Through an Inclined Tube with Different Wave Forms," *Defect and Diffusion Forum*, **392**, 158-177.

Vaidya, H., Rajashekhar, C., Manjunatha, G. and Prasad, K.V. (2019b). "Peristaltic mechanism of a Rabinowitsch fluid in an inclined channel with complaint wall and variable liquid properties," *Journal of the Brazilian Society of Mechanical Sciences and Engineering*, **41**, 52.

Vaidya, H., Rajashekhar, C., Manjunatha, G. and Prasad, K.V. (2019c). "Effect of variable liquid properties on peristaltic flow of a Rabinowitsch fluid in an inclined convective porous channel," *European Physical Journal Plus*, **134**, 231.

Wakif, A., Boulahia, A., Mishra, S. R., Rashidi, M.M. and Sehaqui, R. (2018). "Influence of a uniform transverse magnetic field on the thermo-hydrodynamic stability in water-based nanofluids with metallic nanoparticles using the generalized Buongiorno's mathematical model," *The European Physical Journal Plus*, **133**, 181.

Wakif, A., Boulahia, Z., Amine, A., Animasaun, I.L., Afridi, M.I., Qasim, M. and Sehaqui, R. (2019). "Magneto-Convection Alumina-Water nanofluid within thin horizontal layers using the revised generalized Buongiorno's model," *Frontiers in Heat and Mass Transfer*, **12**, 1-15.

**Received: October 6, 2019**
**Sent to Subject Editor: October 10, 2019**
**Accepted: February 10, 2020**
**Recommended by Subject Editor: Gianfranco Caruso**